

Self-Association of Penicillins in Aqueous Solution as Revealed by Gel Filtration Chromatography

Noriaki FUNASAKI,* Sakae HADA, and Saburo NEYA

Kyoto Pharmaceutical University, Misasagi, Yamashina-ku, Kyoto 607, Japan.

Received November 1, 1993; accepted December 21, 1993

The self-association of penicillin G (PCG) and penicillin V (PCV) in 0.15 M potassium chloride solution has been investigated by frontal gel filtration chromatography (GFC) on Sephadex G-10 columns at 25°C. Analysis of the centroid volume, V_c , of a GFC profile yields the monomer concentration of a penicillin and the weight-average aggregation number, n_w . No critical micelle concentration is observed in the V_c vs. concentration profile for PCV. The n_w value for PCV is 2 at low concentrations and gradually increases with increasing concentration. PCG forms dimers only below 0.06 M, and provides useful GFC data for the investigation of dimerization. The dimerization constants of PCG and PCV are also evaluated from the concentration dependence of the derivative peak position at the trailing boundary. Stepwise aggregation constants, obtained from non-linear least-squares fitting of the centroid volume data, satisfactorily reproduce observed derivative chromatograms, and are used for calculations of the aggregate size distribution of PCV. The structure–association relationship and the effect of self-association on the bactericidal activity and chemical stability of the penicillins are discussed.

Keywords penicillin; self-association; gel filtration chromatography; dimerization

A large number of drugs have been found to self-associate in aqueous media. This behavior plays important roles in the biological and pharmaceutical implications of the drugs. In general, the pharmacological activity of such a drug *in vivo* appears at low concentrations where the self-association of the drug is negligible, but there is a close correlation between the pharmacological activity and self-association property of the drug.¹⁾ For instance, a minimum effective concentration for bactericidal activity by phenothiazines exhibits a linear relation with the micellar aggregation number.²⁾ Many drugs have amphiphilic structures, and some of them begin to self-associate in a small range of concentration. This concentration is called a critical micelle concentration (cmc). The aggregation modes of drugs are classified into two categories, depending on the presence or absence of a cmc; micellar aggregation and non-micellar aggregation. The aggregation mode of a drug is closely related to its chemical structure.¹⁾

Recently, we have developed a gel filtration chromatographic method (GFC) for the investigation of self-association and have carried out a systematic study of the relationship between the aggregation pattern and the chemical structure of a number of compounds, such as methylene blue (MB),³⁾ chlorpromazine hydrochloride (CPZ),⁴⁾ surfactants,^{5,6)} and a zwitterionic derivative of cholic acid (CHAPS).^{7,8)} The major factor for determining the aggregation pattern is the chemical structure of the hydrophobic group. A dye, MB has a planar aromatic ring structure. It has a large dimerization constant and does not have any cmc value.³⁾ The aggregation pattern of a surfactant is characterized not by a single equilibrium between the monomer and the micelle, but by pronounced cooperativity for small aggregates and mild anti-cooperativity for large aggregates.^{5,6)} CHAPS has an aliphatic steroidal structure and exhibits less cooperative self-association than the surfactant.⁷⁾ The driving force for the self-association of these compounds is mainly

hydrophobic interactions, and the repulsion is caused by electrostatic interactions or steric hindrance between the hydrophilic groups at the aggregate surface. The balance between these opposing forces determines the aggregation pattern.⁸⁾

The chemical structures of penicillin G (PCG) and penicillin V (PCV) are shown in Fig. 1. The cmc values and the micellar weight-average aggregation numbers of these penicillins in 0.15 M KCl were determined by static light scattering (Table I).⁹⁾ Interestingly, the bactericidal activity of PCG and PCV against *Escherichia coli* changed critically at 0.134 mM and 0.515 mM, respectively.¹⁰⁾ These concentrations, however, are much lower than their cmc values. Here we can address two questions. Do PCG

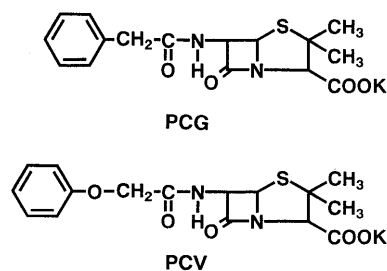


Fig. 1. Chemical Structures of PCG and PCV

TABLE I. Critical Micelle Concentrations, Weight-Average Aggregation Numbers, and Dimerization Constants of Several Self-Associating Compounds at 25.0 °C

Compd.	Added salt	cmc (mM)	n_w	k_{2c} (M^{-1})	k_{2p} (M^{-1})
PCG	0.15 M KCl	300 ^{a)}	2–3 ^{a)}	2.11	2.2
PCV	0.15 M KCl	172 ^{a)}	5–6 ^{a)}	4.38	4.7
CPZ ^{b)}	0.15 M NaCl	4.4–6.4	38	124	118
CHAPS ^{c)}	—	5–10	2–20	4.63	4.7
C ₁₀ E ₈ ^{d)}	—	1.03	46	7.7	7.3

a) Taken from ref. 9. b) Taken from ref. 3. c) Taken from ref. 6. d) Taken from ref. 4.

and PCV not form dimers at much lower concentrations than their cmc values? What is the population of the dimer at the critical concentration for bactericidal activity?

The dimerizing system has a unique derivative chromatogram.^{3,11} Almost all of the self-associating systems form dimers, but the concentration ranges at which dimers only are present are generally limited. From Table I it is expected that PCG is a candidate for such a dimerizing system.

In this work we investigated the self-association behavior of PCG and PCV in 0.15M KCl at 25°C to elucidate the structure-association relationship.

Experimental

Materials Samples of PCG and PCV from Sigma were used as received. Sephadex G-10 from Pharmacia was used according to the procedure suggested by the manufacturer. Blue Dextran (Pharmacia) and potassium chloride of analytical reagent grade were used without further purification. The double-distilled water was degassed immediately before each experiment.

Methods The GFC experiments were carried out on three columns under a flow rate of *ca.* 36 cm³ · h⁻¹. The total volumes of the columns are shown in Table II. The columns were jacketed in order to maintain them at a constant temperature of 25.0 ± 0.2°C. A large volume of sample was applied so that the plateau region appeared on the elution curve. For most cases, the concentration of a penicillin in the eluate was monitored continuously with a differential refractometer detector, and the weight of eluate was also monitored continuously. These concentration and weight data were stored in a computer for further analysis. For cases of PCV at three concentrations (*C*₀ = 0.0300, 0.2002, and 0.2600 M), 2.00 cm³ of eluate was taken in a test tube with a fraction collector, since the refractive index detector did not respond to high concentrations. Each fraction was diluted with 0.15M KCl solution and then the PCV concentration was determined at a wavelength of 266 nm spectrophotometrically. The maximum and minimum on the derivative chromatogram were determined by a polynomial approximation.

The plate theory was employed to simulate the chromatogram. The void volume, *V*₀, and the number, *N*, of plates characteristic of the column are regarded as adjustable parameters. The details of the simulation procedure have already been reported elsewhere.^{8,11}

Results

Evaluation of Aggregation Numbers from Centroid Volumes When a large amount of sample of concentration *C*₀ was applied onto the gel column, a plateau region having the same concentration appeared on the chromatogram. This method, called frontal chromatography, is often used for the investigation of self-associating systems.^{8,12} We may assume that the equivalent sharp boundary for the leading or trailing edge of the solute zone on the frontal chromatogram is approximately the beginning or termination of the plateau region (centroid) of the elution profile and satisfies the relationships^{8,12}:

$$V'_c = \int_0^{C_0} V dC / C_0 \quad (\text{leading boundary}) \quad (1)$$

TABLE II. Some Characteristic Values of the Columns Used and the Number of Data

Compd.	Column	<i>n</i>	<i>V</i> _t (cm ³)	<i>V</i> ₁ (cm ³)	<i>V</i> _m (cm ³)	<i>V</i> _{1g} ⁰ (cm ³)	<i>V</i> _{2g} [∞] (cm ³)	<i>N</i>	<i>V</i> ₀ (cm ³)
PCG	A	8	17.43	17.40	7.05 ^{a)}	16.80	5.21 ^{a)}	21	4.0
PCV	B	9	18.85	24.00	7.03 ^{a)}	23.50	6.35 ^{a)}	30	4.0
PCV	C	7	16.98	21.84	6.35 ^{a)}	—	—	—	—

a) Determined with Blue Dextran.

$$V_c = \int_0^{C_0} V dC / C_0 + S \quad (\text{trailing boundary}) \quad (2)$$

Here *S* denotes the applied volume of the sample. For these determinations the volume coordinate, *V*, is assigned a zero value when the leading boundary of the applied sample enters the column bed. According to this approximation (called asymptotic theory), the elution curve for a non-associable solute is expected to fall within a rectangle of height *C*₀ and width *S*.

Figure 2a shows the frontal chromatogram of PCV at *C*₀ = 0.2002 M on column C. An applied volume of *S* = 42.50 cm³ is greater than the total volume of the column (Table II). The derivative of concentration with respect to the elution volume is shown in Fig. 2b, which will be discussed below. Since two centroid volumes, *V*_c and *V*'_c, obtained from Fig. 2a are close to each other, the average of the two was used for further analysis.

Hereafter, we assume that the equilibria for solute partition between the stationary and mobile phases and for self-association are instantaneously established. When gel pores are smaller than the dimer, one can take the elution volumes of all aggregate species as the void volume of the column.⁸ Under these conditions, from asymptotic theory, we may assume the following equation^{8,12}:

$$V_c = [C_1 V_1 + (C - C_1) V_m] / C \quad (3)$$

Here *V*₁ and *V*_m denote the elution volumes of the monomer and all aggregates including the dimer, respectively, and *C*₁ denotes the monomer concentration. The *V*_c value shown in Fig. 3a is the average of *V*_c and *V*'_c, since they are close to each other within experimental error. Since PCG was slowly hydrolyzed in 0.15M KCl solution, it was very difficult to determine accurate *V*_c values at concentrations higher than the concentration shown in Fig. 3. The values of *V*₁ shown in Table II were estimated by extrapolation of the *V*_c values to *C* = 0. The *V*_m values are set as observed centroid volumes of Blue Dextran on the respective columns. Using these values,

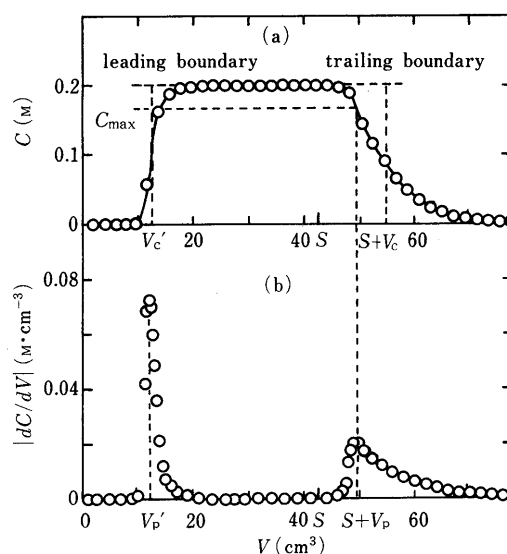


Fig. 2. (a) Frontal Chromatogram and (b) Its Derivative of PCV at *C*₀ = 0.2002 M and *S* = 42.50 cm³

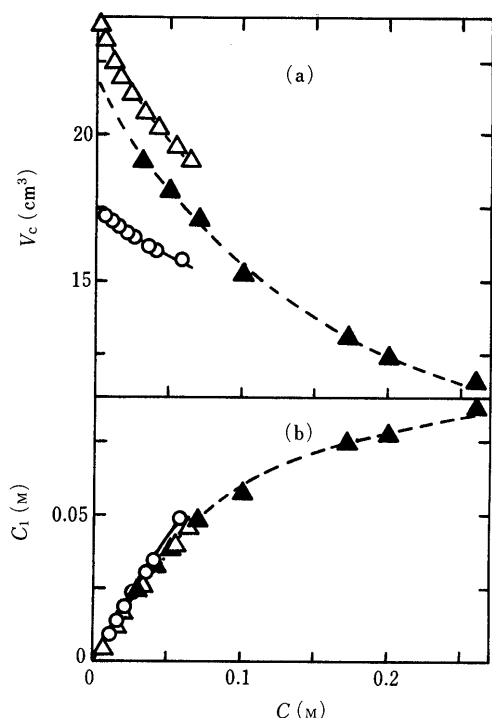


Fig. 3. (a) Centroid Volumes and (b) Monomer Concentrations of PCG (Circles) and PCV (Triangles) Plotted against Total Concentrations, Obtained on Column A (○), Column B (△), and Column C (▲)

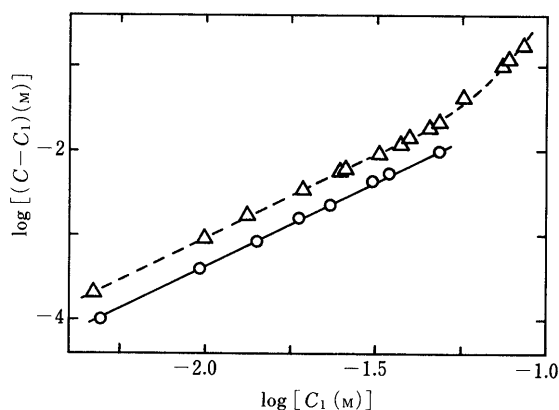


Fig. 4. Double Logarithmic Plots of Monomer Concentrations and Aggregate Concentrations for PCG (○) and PCV (△)

we can estimate the monomer concentration C_1 from Eq. 3. In Fig. 3b, the C_1 values thus obtained for PCG and PCV are shown as a function of the total concentration, C . The monomer concentration of PCV is independent of the columns used.

The concentration dependence of the monomer concentration reflects the aggregation pattern. For the system forming dimers only, we can determine the dimerization constant, k_2 , from

$$k_2 = (C - C_1) / 2C_1^2 \quad (4)$$

The linear portions in Fig. 4 have a slope of $n_w = 2$. From these lines, dimerization constants of 2.10 and 4.34 M^{-1} were evaluated for PCG and PCV, respectively. From the concentration dependence of C_1 , we can estimate the weight-average aggregation number, n_w , from⁸⁾

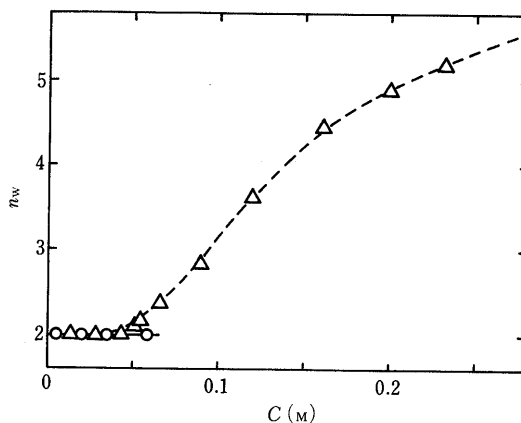


Fig. 5. Weight-Average Aggregation Numbers of PCG (○) and PCV (△)

The solid and dashed lines are calculated on the basis of model VI-1 of PCG and model V-4 of PCV, respectively.

$$n_w = d \log (C - C_1) / d \log C_1 \quad (5)$$

This equation holds true for self-associating systems, irrespective of the kind and concentration of aggregates. From the slope of the plot of $\log (C - C_1)$ vs. $\log C_1$, shown in Fig. 4, we can estimate n_w as a function of the total concentration for PCG and PCV. As Fig. 5 shows, the weight-average aggregation number of PCV increases continuously with increasing concentration, and that of PCG remains constant at 2 within the concentration range investigated.

Derivative Elution Profiles The derivative of a frontal chromatogram with respect to the elution volume, V , can provide some information about the properties of self-associating systems. The derivative chromatograms at low concentrations of PCG and PCV are shown in Fig. 6. For the sake of direct comparison, the chromatograms for the trailing boundary are shown against the volume coordinate of elution volume V minus applied volume S . For the self-associating system, generally, the trailing boundary spreads more than its leading counterpart.⁸⁾ As Fig. 6 shows, self-association occurs at concentrations much lower than the cmc for both PCG and PCV. This result differs remarkably from those of the nonionic surfactants.^{5,6)} When compared at close concentrations, the gap between the heights of the leading and trailing peaks is larger for PCV than for PCG. This result suggests that the dimerization constant for PCV is larger than that for PCG.

According to asymptotic theory, the volume, V_p , of the trailing monomer peak for the dimerization system approximately obeys the following equation^{8,11,13)}:

$$\{(V_{1p}^0 - V_{2p}^\infty) / (V_p - V_{2p}^\infty)\}^2 = 1 + 9.6k_2 C_{\max} \quad (6)$$

where C_{\max} denotes the concentration at V_p (Fig. 2b). As Fig. 6 shows, the V_p value decreases with increasing concentration. The V_{1p}^0 value may be estimated from extrapolation of the V_p values to zero concentration, and the V_{2p}^∞ value may be set as the V_p value of Blue Dextran. These values are included in Table II. In Fig. 7, the observed V_p values are plotted according to Eq. 6. The C_{\max} values are greater than half of the respective total

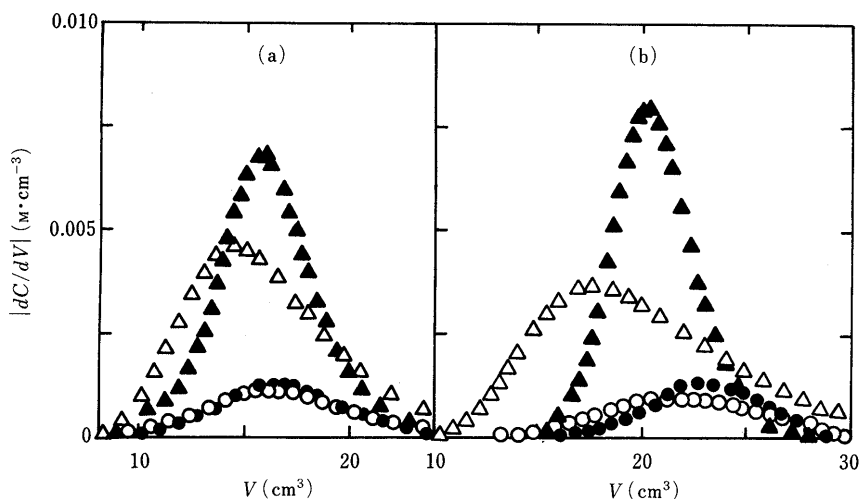


Fig. 6. Observed Derivative Chromatograms at the Leading (Closed Symbols) and Trailing (Open Symbols) Boundaries for (a) PCG and (b) PCV. The applied concentrations (M) of PCG: \circ , \bullet , 0.01006; \triangle , \blacktriangle , 0.04003. The applied concentrations (M) of PCV: \circ , \bullet , 0.01057; \triangle , \blacktriangle , 0.04177.

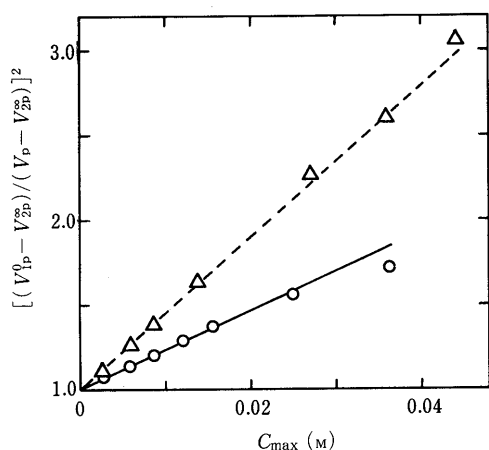


Fig. 7. Plots According to Eq. 6 for PCG (\circ) and PCV (\triangle)

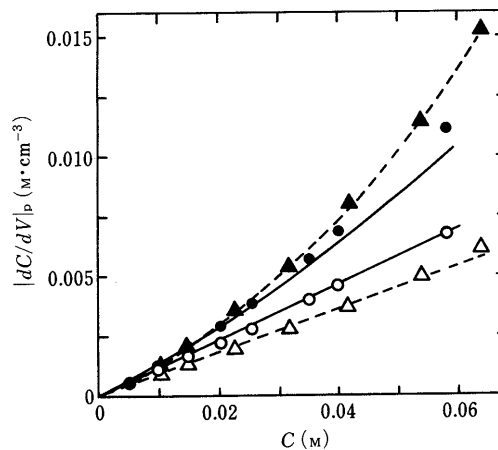


Fig. 8. Peak Heights at the Leading (Closed Symbols) and Trailing (Open Symbols) Boundaries Plotted against the Applied Concentrations of PCG (Circles) and PCV (Triangles) on Column B

The solid and dashed lines are calculated on the basis of model VI-1 of PCG and model V-4 of PCV, respectively.

$$K_i = [A_i]/C_1^i \quad (8)$$

These equilibrium constants can be connected by

$$K_i = \prod_2^i k_i \quad (9)$$

concentrations. As Fig. 5 shows, PCG and PCV form dimers only at low concentrations. The application of Eq. 6 to the V_p data at these low concentrations yields the dimerization constants of PCG and PCV. These k_{2p} values, shown in Table I, are close to the k_{2c} values.

For self-associating systems, generally, the peak at the leading boundary is higher than that at the trailing boundary.⁸⁾ Figure 8 shows the peak heights at the leading and trailing boundaries as a function of the total concentration. For both PCG (column A) and PCV (column B), the trailing peak height is almost proportional to the total concentration. This is an important result for the investigation of self-association by GFC. The solid and dashed lines are theoretically calculated on the basis of the models stated below.

Aggregation Models and Predictions of Some Aggregation Properties When the i -mer (A_i) is in equilibrium with the $(i-1)$ -mer and monomer, one can define the stepwise aggregation constant, k_i , as

$$k_i = [A_i]/([A_{i-1}]C_1) \quad (7)$$

When i -mer is formed from i monomers, one can define the one-step (or overall) aggregation constant, K_i , as

The aggregation pattern is quantitatively expressed by the dependence of k_i or K_i on i . Hereafter we will apply five models which take into consideration all aggregate species and give analytical expressions for the total concentration C as a function of the monomer concentration C_1 .

In model I, we assume a series of equations, $k_2 \neq k_3 \neq \dots \neq k_{i-1} \neq k_i = k_{i+1} = \dots = k$; that is, aggregation occurs isodesmically when the aggregation number is large. Then we can write the total concentration C as a function of C_1 :

$$C = C_1 + 2k_2 C_1^2 + \dots + (i-1)K_{i-1} C_1^{i-1} + K_{i-1} k C_1^i \{i - (i-1)k C_1\} / (1 - k C_1)^2 \quad (10)$$

The weight-average aggregation numbers, n_w , can be also

calculated from this model.

In model II, we assume a marked attenuation (anti-cooperativity) of k_i at large aggregation numbers. Such an attenuation is caused by the steric or electrostatic repulsion between the head groups at the aggregate surface and often leads to the termination of growth of the aggregate size at high concentrations. When $k_2 \neq k_3 \neq \dots \neq k_{i-1} \neq k_i$ and $ik_i = (i+1)k_{i+1} = \dots = k$, one can write C as

$$C = C_1 + 2k_2 C_1^2 + \dots + (i-1)K_{i-1} C_1^{i-1} + (i-1)! K_{i-1} C_1 / k^{i-2} \{ \exp(kC_1) - 1 - kC_1 - (kC_1)^2/2! - \dots - (kC_1)^{i-2}/(i-2)! \} \quad (11)$$

In model III, we assume a mild attenuation of k_i with an increasing aggregation number at large aggregation numbers. When $k_2 \neq k_3 \neq \dots \neq k_{i-1} \neq k_i$ and $(i-1)k_i/i = ik_{i+1}/(i+1) = \dots = k$, one can write C as

$$C = C_1 + 2k_2 C_1^2 + \dots + (i-1)K_{i-1} C_1^{i-1} + K_{i-1} k C_1^i \{ i^2 - (2i^2 - 2i - 1)kC_1 + (i-1)^2 (kC_1)^2 \} / \{ (i-1)(1 - kC_1)^3 \} \quad (12)$$

In model IV, we assume a mild increase (cooperativity) of k_i with an increasing aggregation number at large aggregation numbers; $k_2 \neq k_3 \neq \dots \neq k_{i-1} \neq k_i$ and $ik_i/i = (i-1)k_{i+1}/(i+1) = \dots = k$. Then we can write C as

$$C = C_1 + 2k_2 C_1^2 + \dots + (i-1)K_{i-1} C_1^{i-1} + (i-1)K_{i-1} k C_1^i / (1 - kC_1) \quad (13)$$

In model V, we assume that, according to the Tanford theory for micellization of surfactants,^{6,14} the standard Gibbs energy ΔG_i^0 of i -mer formation from i monomers can be written as

$$i\Delta G_i^0/RT = -ai + bi^{2/3} + ci^{4/3} \quad (14)$$

Then, the molarity, C_i , of i -mer can be represented as a function of monomer concentration C_1 by

$$C_i = C_1^i \exp(-i\Delta G_i^0/RT) \quad (15)$$

and the total concentration is

$$C = C_1 + 2k_2 C_1^2 + \dots + (i-1)K_{i-1} C_1^{i-1} + \sum_{j=i}^{\infty} j C_1^j \exp[-(-aj + bj^{2/3} + cj^{4/3})] \quad (16)$$

In model VI, a single aggregate species i is assumed to

be in equilibrium with the monomer. The total concentration can be written as

$$C = C_1 + iK_i C_1^i \quad (17)$$

The observed monomer concentration data (Fig. 3b) may be considered to be fitted to models I—VI. These data, however, are not primarily determined by the experiments and their uncertainties are dependent on the total concentration. From this viewpoint we employ the V_c data to be best-fitted to the aggregation models. Thus, we use Eq. 3 and one of Eqs. 10—13, 16, and 17, together with the observed values of V_1 and V_m (Table II); that is, the SS value for V_c is minimized:

$$SS = \sum_1^n (V_{c, \text{calc}} - V_{c, \text{obsd}})^2 \quad (18)$$

Here n denotes the number of V_c data ($n=8$ for PCG and $n=16$ for PCV). To best-fit stepwise aggregation constants, we need rough initial values for them. In the same manner as already reported for CHAPS,⁷ we obtained the best-fit aggregation constants for PCV based on model I. The number of independent parameters is increased until the SS value does not decrease further.

For instance, the stepwise aggregation constants of model I were fitted to the observed V_c values as follows: First, the two values, k_2 and k , only were regarded as independent parameters in Eq. 10 ($i=3$). As the initial values of k_2 and k , we employed the k_2 value estimated from the linear portion of Fig. 4. Then the monomer concentration C_1 at a given total concentration was calculated from Eq. 10 by the Newton-Raphson method,¹⁵ and the V_c value was from Eq. 3 at the total concentration. The values of V_c were also calculated at all total concentrations ($n=16$) where the GFC experiments were carried out. The initial SS value was calculated from Eq. 18. Better values of k_2 and k were searched for by a non-linear least-squares method.¹⁶ The best-fit values of k_2 and k were obtained after repetition of the above procedure. Secondly, the values of k_2 , k_3 , and k were regarded as independent parameters in Eq. 10 ($i=4$). As the initial values of k_3 and k , we employed the best-fit k value determined above, and the above calculations were repeated to obtain the best-fit values of k_2 , k_3 , and k for this three-parameter model. Finally, the best-fit values of six aggregation constants were determined for model I-6 shown in Table III. The reliability of the best-fit values of

TABLE III. Best-Fit Values of Stepwise Aggregation Constants for PCV

Model	SS (cm ⁶)	AIC ^a	k_2 (M ⁻¹)	k_3 (M ⁻¹)	k_4 (M ⁻¹)	k_5 (M ⁻¹)	k_6 (M ⁻¹)	k (M ⁻¹)	a	b	c
I-6	0.2801	-8.36	4.35 (0.16) ^b	0.0014 (0.0013)	16.5 (6.8)	630 (19)	361 (21)	5.8 (4.7)	—	—	—
II-6	0.2785	-8.45	4.34 (0.16)	0.0015 (0.0014)	16.5 (15.8)	630 (47)	361 (19)	41 (17)	—	—	—
III-6	0.2785	-8.45	4.35 (0.16)	0.0047 (0.0069)	8 (13)	113 (17)	1269 (48)	4.9 (4.7)	—	—	—
IV-6	0.2802	-8.36	4.35 (0.15)	0.0025 (0.0021)	29 (21)	143 (30)	520 (28)	6.3 (5.1)	—	—	—
V-4	0.2700	-12.95	4.38 (0.12)	—	—	—	—	—	78.2 (0.8)	75.8 (1.1)	19.3 (0.3)

^a Akaike's information criterion (AIC) is defined as: $AIC = n \ln SS + 2m$. Here m stands for the number of adjustable parameters (H. Akaike, *IEEE Trans. Automat. Contr.*, 19, 716 (1974)).¹⁶ ^b The value in the parenthesis is the standard deviation of the best-fit value.

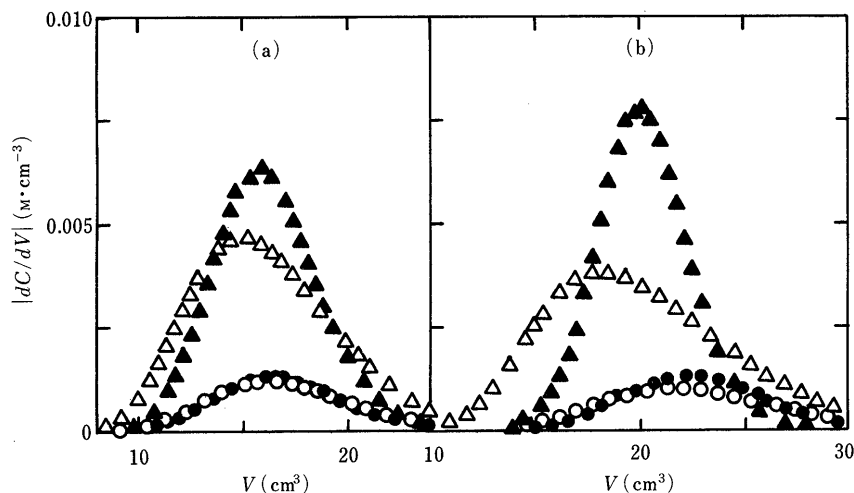


Fig. 9. Simulated Derivative Chromatograms Based (a) on Model VI-1 for PCG and (b) on Model V-4 for PCV. The symbols are the same as those in Fig. 6.

k_3 , k_4 , and k is not very high, as assessed from their standard deviations.

Table III summarizes the best-fit parameters for models I—V of PCV. The Arabic numeral of each model denotes the number of adjustable parameters. The best-fit values of K_i and i for model VI-2 are $22.9 \pm 9.4 (\text{M}^{-1})^{-1.52}$ and 2.52 ± 0.15 , and SS is equal to 3.200 cm^6 . Thus, model V-4 is the best for PCV. For PCG, the dimerization constant is regarded as the adjustable parameter, since only the dimer is present in the concentration range investigated (Fig. 5). The best-fit dimerization constant for PCG is $2.11 \pm 0.04 \text{ M}^{-1}$ and $SS = 0.011 \text{ cm}^6$. This will hereafter be termed model VI-1 of PCG.

The above aggregation models can be used to predict a number of chromatographic and aggregation properties which may or may not be obtained by the experiment. In Fig. 3, the solid lines for the centroid volume and the monomer concentration are calculated on the basis of model VI-1 of PCG and the dashed lines are based on model V-4 of PCV. As expected, the agreement between theory and experiment is excellent.

The concentration of each aggregate species of PCV can be calculated on the basis of any of aggregation models I—V by using the monomer concentration and the stepwise aggregation constants shown in Table III. From this concentration we can calculate the weight-average aggregation number, n_w , as a function of the total concentration. The solid lines shown in Fig. 5 are calculated on the basis of model VI-1 of PCG and the dashed lines are based on model V-4 of PCV. These theoretical lines well reproduced the observed n_w values for PCG and PCV.

The derivative chromatograms shown in Fig. 9 are simulated on the basis of model V-4 of PCV and model VI-1 of PCG together with plate theory for chromatography.⁸⁾ The void volume, V_0 , and the number, N , of plates for this theory are regarded as adjustable parameters. The employed values of V_0 and N are shown in Table II. The derivative chromatogram of PCV at $C_0 = 0.2002 \text{ M}$ (Fig. 2b) is also reproduced on the basis of model V-4 very well (data not shown). The solid and

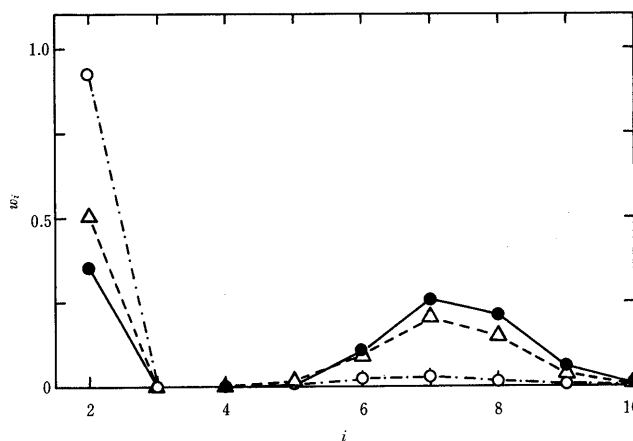


Fig. 10. Aggregate Size Distributions of PCV, Calculated on the Basis of Model V-4 at Three Concentrations (M): \circ , 0.06421; \triangle , 0.1722; \bullet , 0.2600

dashed lines in Fig. 8 are based on model VI-1 of PCG and model V-4 of PCV, respectively. The agreement between theory and experiment (Figs. 8 and 9) is very good, suggesting that these models well reproduce the aggregation patterns of PCG and PCV.

The weight fraction, w_i , of i -mer in all aggregate species (excluding the monomer) is defined as

$$w_i = i[A_i] / \sum_{i=2}^{\infty} i[A_i] = i[A_i] / (C - C_1) \quad (19)$$

The weight fraction of the i -mer of PCV, calculated on the basis of model V-4, is shown as a function of i in Fig. 10. At low concentrations the dimer is the predominant aggregate species and the heptamer is the most probable aggregate species at high concentrations. The other models shown in Table III predict similar size distributions.

Discussion

The present results clearly show that PCV self-associates stepwise without any cmc. If PCV has any cmc, the trailing derivative chromatograms at concentrations higher than

the cmc should be bimodal.⁸⁾ Although such a bimodality was found for nonionic surfactants^{5,6)} and CPZ,⁴⁾ it was not observed for PCV (e.g. see Fig. 2b). At high concentrations of PCV, the heptamer is the major aggregate. Further growth of aggregates will be hampered by electrostatic repulsion between the carboxylate ions at the aggregate surface. These aggregation patterns of PCV are rather similar to those of CHAPS,⁷⁾ probably since these compounds both have aliphatic cyclic structures. The major difference is that CHAPS self-associates more cooperatively than PCV.

The dimerization constants of PCV and PCG are determined from the V_c and V_p data independently. Furthermore, the observed derivative chromatograms (Fig. 6) are well reproduced at low concentrations (Fig. 9) where the dimers are the predominant aggregates (Fig. 10). These results indicate that the dimerization constants shown in Table I are reliable. These dimerization constants are small compared with those of other compounds. PCV appears to be more hydrophobic than PCG, when their values of n_w , cmc, and k_2 are compared (Table I). Furthermore, since V_{1p}^0 and V_1 of PCV are larger than V_1 (Table II), the monomer of PCV is adsorbed onto the Sephadex gel. The monomer of PCG is retained mainly by the molecular sieve mechanism (Table II). This result also indicates the difference in hydrophobicity between PCG and PCV. The retention mechanisms of self-associating compounds have already been reported.¹⁷⁾

The bactericidal activity of PCG increases rapidly with increasing PCG concentration below 0.134 mM, but the activity levels off above this concentration.¹⁰⁾ At this concentration, the molarity of the PCG dimer is 3.8×10^{-5} mM and this amounts to 0.0060% of the total weight of PCG. The critical concentration of bactericidal activity of PCV is 0.515 mM,¹⁰⁾ at which 0.45% of PCV dimerizes. Thus, the dimerization of PCG and PCV does not seem to be responsible for the critical changes in bactericidal activity. Since penicillins are slowly hydrolyzed in aqueous solutions, their concentrated solution, stored in a refrigerator, is diluted by physiological saline solution immediately before injection.¹⁸⁻²⁰⁾ The hydrolysis rate of PCG is increased markedly by self-association.^{20,21)} Each GFC experiment of PCG finished within about 3 h and the maximum PCG concentration used is 0.058 M. Under these conditions, less than 0.3% of PCG was hydrolyzed.²¹⁾ The hydrolysis of PCV was negligible.^{18,19,21)} Since we used potassium salts of PCG and PCV in the present work, we used potassium chloride as the added salt, instead of sodium chloride.

Since PCG and PCV have small dimerization constants and high cmc values, they are compounds suitable for

the study of GFC methodology of dimerization. For a non-associable solute, we have shown that both derivative peak heights at the leading and trailing boundaries are directly proportional to the concentration applied. At the trailing boundary on the derivative chromatogram, dimerization exhibits unimodality, but the other multimerizations exhibit bimodality.^{8,13)} The trailing peak position follows Eq. 6 (Fig. 7). From these results, we can expect that the trailing peak height is directly proportional to the total concentration. In fact, both the observed and calculated heights of the trailing peak are proportional to the total concentration for PCG and PCV (Fig. 8), but this is not true for the leading peak height. The height ratio of the leading peak to the trailing peak appears to relate to the dimerization constant; this ratio is larger for PCV than for PCG, since the dimerization constant of PCV is larger than that for PCG (Table I). The present results will be applicable to dimerization and higher multimerizations of other compounds.

Acknowledgment Thanks are due to Misses Tomoko Mitsunaga, Megumi Mizukawa, Noriko Kagawa, and Hiroko Gokan for their help with the GFC experiments.

References

- 1) D. Attwood, A. T. Florence, "Surfactant Systems," Chapman and Hall, London, 1984, Chapter IV.
- 2) A. T. Florence, *Adv. Colloid Interface Sci.*, **2**, 115 (1968).
- 3) S. Hada, S. Neya, N. Funasaki, *Bull. Chem. Soc. Jpn.*, **65**, 314 (1992).
- 4) N. Funasaki, S. Hada, J. Paiement, *J. Phys. Chem.*, **95**, 4131 (1991).
- 5) N. Funasaki, H.-S. Shim, S. Hada, *J. Chem. Soc., Faraday Trans.*, **87**, 957 (1991).
- 6) N. Funasaki, H.-S. Shim, S. Hada, *J. Phys. Chem.*, **96**, 1998 (1992).
- 7) N. Funasaki, S. Hada, S. Neya, *J. Phys. Chem.*, **95**, 1846 (1991).
- 8) N. Funasaki, *Adv. Colloid Interface Sci.*, **43**, 87 (1993).
- 9) D. Attwood, S. P. Agarwal, *J. Pharm. Pharmacol.*, **36**, 563 (1984).
- 10) G. N. Rolinson, *Proc. Roy. Soc. London*, **B163**, 417 (1966).
- 11) N. Funasaki, S. Hada, S. Neya, *Bull. Chem. Soc. Jpn.*, **67**, 65 (1994).
- 12) G. K. Ackers, *Adv. Protein Chem.*, **24**, 343 (1970).
- 13) G. K. Ackers, T. E. Thompson, *Proc. Natl. Acad. Sci. U.S.A.*, **53**, 342 (1965).
- 14) C. Tanford, "The Hydrophobic Effect," John Wiley, New York, 1980, Chapter VII.
- 15) R. G. Mortimer, "Mathematics for Physical Chemistry," Macmillan, New York, 1981, p. 249.
- 16) K. Yamaoka, "Analysis of Pharmacokinetics with Microcomputers," Nankodo, Tokyo, 1984, Chapter II.
- 17) N. Funasaki, S. Hada, S. Neya, *J. Colloid Interface Sci.*, **156**, 518 (1993).
- 18) J. P. Hou, J. W. Poole, *J. Pharm. Sci.*, **60**, 503 (1971).
- 19) P. C. van Krimpen, W. P. van Bennekom, A. Bult, *Pharm. Weekbl. Sci. Ed.*, **9**, 1 (1987).
- 20) J. H. Ong, H. B. Kostenbauer, *J. Pharm. Sci.*, **64**, 1378 (1975).
- 21) N. Funasaki, S. Hada, S. Neya, in preparation.